Solving Minimum Dynamic Residual Expansion and Using Results for Error Localization

Adrien Bobillot and Etienne Balmès

ECOLE CENTRALE PARIS
MSSMat
Châtenay Malabry Cedex, 92295 FRANCE
bobillot@mss.ecp.fr, balmes@mss.ecp.fr

ABSTRACT

Minimum Dynamic Residual Expansion (MDRE) seeks to estimate the response of test modeshapes at all degrees of freedom of a model by minimizing the weighted sum of a test error defined at sensors and a modeling error taken to be the strain energy of the dynamic residual associated with the estimated modeshape. Theoretically the computation of the dynamic residual gives a simple mechanism to localize modeling errors. While various forms of MDRE have been often considered in the literature, few systematic analyses of the exact resolution have been attempted on industrial models in good part because of excessive computational costs. The present paper introduces an iterative method allowing the exact solution of MDRE for large problems. Exact solutions, either direct or iterative, are compared with reduced basis versions that were proposed in earlier papers. The ability to localize errors is then evaluated for simulated tests with known modifications. The evaluations are shown for a small 1032 DOF model of the GARTEUR SM-AG-19 testbed and a more industrial 16840 DOF model of an engine cover.

1 INTRODUCTION

Expansion methods seek to estimate the motion at all DOFs of a FE model based on information known at sensors. A classification of expansion methods was proposed in Ref.[7] dividing methods into subspace based, where the model is used to build the subspace in which the expanded modes will lay, and error based where modeling and measurement errors are considered simultaneously. Well known subspace methods are modal [1]/SEREP [2], static (based on Guyan reduction [3]), dynamic [4] and hybrid [5] [6].

Error based expansion methods (see [7] [8] among others) have rarely been applied to industrial size models due to excessive computational costs. This paper introduces an exact iterative resolution technique which enables detailed studies of this class of methods. Section 2 goes through various formulations of Minimum Dynamic Residual Expansion (MDRE) and relates those to practical solution strategies including the new exact iterative method. Convergence of the solution is analyzed in section 3.

Finally, the motivation typically set forth for solving MDRE problems is that the displacement residual associated with the modeling error should enable localization of modeling errors. The ability to actually do so is analyzed in detail in section 4.

2 MINIMUM DYNAMIC RESIDUAL EXPANSION

2.1 Motivations

Minimum dynamic residual expansion methods estimate responses at all DOFs of the FE model by formulating a minimization problem combining modeling and measurement errors.

Measurement errors are taken into account using a quadratic norm

$$\epsilon_j = \|\{y_{Test,j}\} - [c]\{\phi_{exp,j}\}\|^2_{Q_j} \tag{1}$$

where the Q_j norm can be used to weight the different sensor responses according to their reliability. Using such a norm, that takes into account an estimated relative error on measurements, seems most appropriate. Various energy based metrics have also been considered in [8] although the physical significance of an energy norm on test results is unclear.

Modeling errors are taken into account using the energy norm of a residual. Natural dynamic residuals are $R_{L,j} = Z(\omega_j)\phi_j$ for modeshapes and $R_{L,j} = Z(\omega_j)\{q\} - F$ for frequency response functions. These residuals correspond to generalized loads. To obtain an energy norm, they must be associated to displacement residuals. The standard solution [9] is to compute the static response to the dynamic load residual

$$R_{D,j} = \hat{K}^{-1} R_{L,j}, \tag{2}$$

where $\hat{K}$ is the stiffness of a nominal FE model and can be a mass-shifted stiffness in the presence of rigid body modes. Mod-

eling error is thus estimated using the associated strain energy

$$\|R_{D,j}(\phi_{exp})\|_K^2 = \{R_{D,j}\}^T[K]\{R_{D,j}\}. \quad (3)$$

Given metrics on test and modeling error, one uses a weighted sum of the two types of errors to formulate a generalized least-squares problem, where one seeks to minimize the cost function

$$J(\omega_{Test,j}) = \min_{\phi_{exp,j}} \big(\|R_D(\phi_{exp,j})\|_K^2 + \gamma_j \epsilon_j \big). \quad (4)$$

In the applications shown, the relative weight γ_j of the two terms is varied until a preselected level of measurement error is reached

$$\frac{\|\{y_{Test,j}\} - [c]\{\phi_{exp,j}\}\|_{Q_j}}{\|\{y_{Test,j}\}\|_{Q_j}} = \sigma_j, \quad (5)$$

with σ_j the relative error on the measured mode $y_{Test,j}$.

Choosing to fix σ_j is somewhat arbitrary. Saying there is 1% or 10% error on the measured vector seems a reasonable statement. Using a vector norm on the error will correctly account for the fact that locations of high response are usually identified with less error. But until methods to estimate bias and variance on modeshapes are developed, the indicator used to quantify measurement error will remain arbitrary.

2.2 Two-field formulation

The load and displacement residuals verify $[K]\{R_D, j\} - [Z(\omega_{Test,j})]\phi_{exp,j} = 0$. Using a Lagrange multiplier λ_j to enforce this relation, one can reformulate problem (4) as

$$\begin{aligned} J(\omega_{Test,j}) = \min_{R_{D,j},\phi_{exp,j},\lambda} & \big(\{R_{D,j}\}^T K \{R_{D,j}\} \\ & + \gamma_j \|[c]\phi_{exp,j} - y_{Test,j}\|_{Q_j}^2 \\ & + \lambda_j \|K.\{R_{D,j}\} - Z(\omega_{Test,j})\phi_{exp,j}\|^2 \big). \end{aligned} \quad (6)$$

At the optimum, the derivative of (6) with respect to $R_{D,j}$, $\phi_{exp,j}$ and λ_j should be zero, so that

$$\begin{bmatrix} K & 0 & K \\ 0 & \gamma_j c^T Q_j c & -Z_j \\ K & -Z_j & 0 \end{bmatrix} \begin{Bmatrix} R_{D,j} \\ \phi_{exp,j} \\ \lambda \end{Bmatrix} = \begin{Bmatrix} 0 \\ \gamma_j c^T Q_j y_{Test,j} \\ 0 \end{Bmatrix} \quad (7)$$

with $Z_j = Z(\omega_{Test,j})$.

By remarking that the first two blocks give $\lambda = -R_{D,j}$, one can actually solve a two field $(R_{D,j}, \phi_{exp,j})$ formulation (see also [10])

$$\begin{bmatrix} -K & Z_j \\ Z_j & \gamma_j c^T Q_j c \end{bmatrix} \begin{Bmatrix} R_{D,j} \\ \phi_{exp,j} \end{Bmatrix} = \begin{Bmatrix} 0 \\ \gamma_j c^T Q_j y_{Test,j} \end{Bmatrix}. \quad (8)$$

Formulation (8) is similar to (4), except there no longer is a need to define a mass shift.

2.3 Reduced basis version

The reduced basis resolution of (7) implies the choice of a reduction basis for $\{\phi_{exp,j}\}$ and $R_{D,j}$. The simplest alternative is to take the same bases for these two fields, that is

$$\begin{Bmatrix} \hat{R_{D,j}} \\ \hat{\phi_{exp,j}} \end{Bmatrix} = \begin{Bmatrix} T R_{red,D,j} \\ T \phi_{red,exp,j} \end{Bmatrix}, \quad (9)$$

and in this case the reduced basis version of (8) is

$$\begin{bmatrix} T^T K T & T^T Z_j T \\ T^T Z_j T & \gamma_j T^T c^T Q_j c T \end{bmatrix} \begin{Bmatrix} R_{red,j} \\ \phi_{red,exp,j} \end{Bmatrix} = \begin{Bmatrix} 0 \\ \gamma_j T^T c^T Q_j y_{Test,j} \end{Bmatrix} \quad (10)$$

The bases proposed in [7], and used in section 3.2, combine nominal modes, static responses associated with sensors, ...

2.4 Iterative solution of exact problem

The reduced solution (10) being an estimate of the exact solution, a procedure to enrich T iteratively is proposed here. The procedure computes residuals to evaluate the accuracy of the reduced solution and, if needed, adds displacement residuals to the reduction basis. These residuals are defined as

$$\begin{Bmatrix} R_{L,R_D,j} \\ R_{L,\phi,j} \end{Bmatrix} = \begin{bmatrix} -K & Z_j \\ Z_j & \gamma_j c^T Q_j c \end{bmatrix} \begin{Bmatrix} \hat{R_{D,j}} \\ \hat{\phi_{exp,j}} \end{Bmatrix} - \begin{Bmatrix} 0 \\ \gamma_j c^T Q_j y_{Test,j} \end{Bmatrix}. \quad (11)$$

The procedure for the completion of T is then based on the estimation of the relative strain energy of $R_{L,R_D,j}$ and $R_{L,\phi,j}$. At iteration n, the following steps are performed:

1. Computation of the load residuals $R_{n,L,R_D,j}$ and $R_{n,L,\phi,j}$ associated to the basis T_n (see (11)),
2. Computation of the displacement residuals

$$\begin{aligned} R_{n,D,R_D,j} &= \hat{K}^{-1} R_{n,L,R_D,j} \\ R_{n,D,\phi,j} &= \hat{K}^{-1} R_{n,L,\phi,j}, \end{aligned} \quad (12)$$

3. Evaluation of the relative strain energy errors,

$$\begin{aligned} \epsilon_{n,R_D,j} &= \frac{R_{n,D,R_D,j}^T K R_{n,D,R_D,j}}{\hat{R_{D,j}}^T K \hat{R_{D,j}}} \\ \epsilon_{n,\phi,j} &= \frac{R_{n,D,\phi,j}^T K R_{n,D,\phi,j}}{\hat{\phi_{exp,j}}^T K \hat{\phi_{exp,j}}}, \end{aligned} \quad (13)$$

4. Completion

$\epsilon_{n,R_D,j} > Tol \Rightarrow T_{n+1} = [T_n, \{R_{D,R_D,j}\}]$

$\epsilon_{n,R_\phi,j} > Tol \Rightarrow T_{n+1} = [T_n, \{R_{D,\phi,j}\}]$

These steps are repeated until every ϵ_j is less than a user-fixed tolerance (typically 10^{-8} for high precision).

It should be noted that many normalization problems arise from adding residuals to the basis T_n, which is typically composed of modes, mode sensitivities and static responses to unit loads at

sensors. Indeed, residuals are of a different type from T_n, do not necessarily have the same order of magnitude, and can also be very colinear to the space spanned by T_n. All these causes lead to numerical conditioning problems that need proper treatment to achieve convergence.

3 SOLVING MDRE PROBLEM

3.1 Models used for applications

The expansion process exposed in section 2 has been tested on two models. Except for importing the element matrix dictionary of the engine cover from NASTRAN, all computations were performed using the Structural Dynamics Toolbox for MATLAB[11].

The first model, the GARTEUR SM-AG-19 testbed used as a benchmark by the COST F3 working group on model updating, has 1032 DOFs. Its sensor configuration is shown on figure 1. Sensors do not necessarily coincide with Finite Element (FE) DOFs, so that motion at sensors is interpolated using an elaborate technique (rigid links shown as thick lines in figure 1 with interpolated rotations using nodes shown with circles). The method has been tested with simulated experimental modes. Simulated experimental modes are generated by introducing a stiffness modification in a substructure (see figure 1) $K_{mod} = 2K_{mod,0}$. The modes of that modified structure are then computed and projected on the sensors DOFs, which gives "simulated experimental modes".

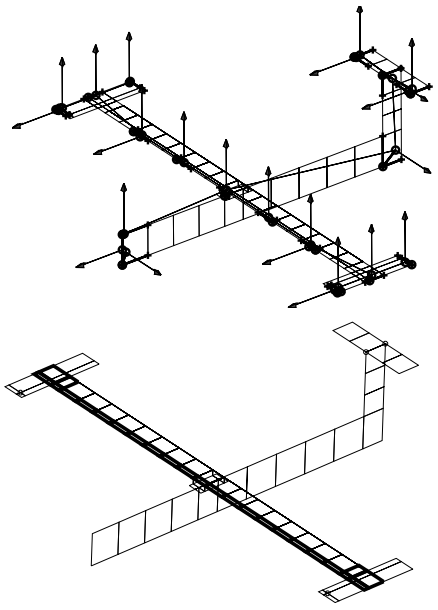

Figure 1: Top: Sensor configuration of garteur and links used to observe motion at sensor locations, Bottom: Localization of the modification $K_{mod} = 2K_{mod,0}$

The second, more industrial model, is an engine cover model with 16840 DOFs. The sensor wire-frame representation and the sensor measurement directions are shown in figure 2. The technique previously mentioned is also applied here to estimate motion at sensors. The modification introduced is a stiffness perturbation ($K_{mod} = .5K_{mod,0}$ for the central part of the cover, plotted in bold in figure 2).

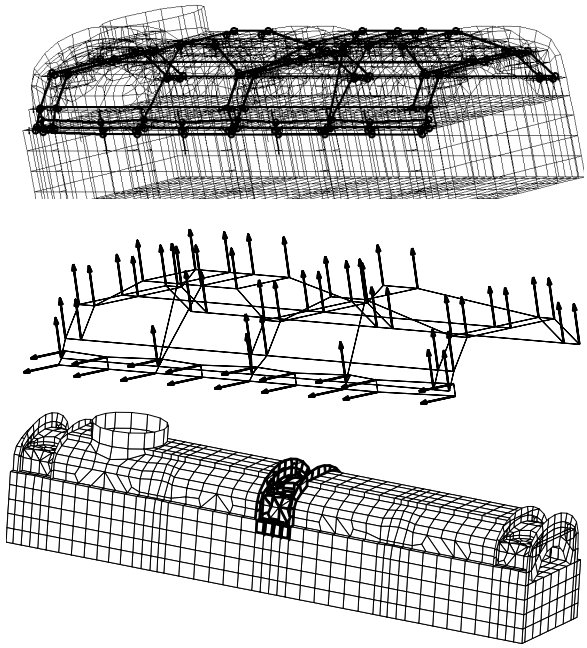

Figure 2: Top: Wire-frame representation of the sensors (sensors located at bold points) for the engine cover, Middle: Sensor measurement directions, Bottom: Localization of modification $K_{mod} = .5K_{mod,0}$

3.2 Comparing solutions

The objective of this section is to compare the methods proposed in section 2 with respect to their accuracy and computational efficiency. The considered bases are

- Modal: $T_{mod} = [\phi_{nom,1:20}]$ computed for the nominal structure.
- modal + static responses to unit loads at sensors: $T_{mod+stat} = \left[\phi_{nom,1:20}, \hat{K}^{-1}c^T\right]$ where c is the observation matrix associated to the sensors.
- modal + sensitivities: $T_{mod+sens} = \left[\phi_{nom,1:20},\ \frac{\partial\phi}{\partial p}_{7:20}\right]$, where sensitivities of the flexible modes are computed with respect to the parameter corresponding to the modification introduced.
- modal + sensitivities + static responses: $T_{mss} = \left[\phi_{nom,1:20},\ \frac{\partial\phi}{\partial p}_{7:20},\ \hat{K}^{-1}c^T\right]$.
- exact iterative : T_{enr} which is the basis T_{mss} enriched by the iterative procedure described in 2.4 with $\gamma = 10^8$ and a tolerance set to 10^{-8}.

The two applications have been chosen so that the exact direct solution (8) could be computed. For accuracy, the comparisons use a relative strain energy error to establish the validity of expanded modeshapes

$$\alpha_j = \frac{\{\phi_{exa,j} - \phi_{red,j}\}^T K \{\phi_{exa,j} - \phi_{red,j}\}}{\{\phi_{exa,j}\}^T K \{\phi_{exa,j}\} + \{\phi_{red,j}\}^T K \{\phi_{red,j}\}} \quad (14)$$

and of the displacement residuals defined in (9)

$$\beta_j = \frac{\left\{\hat{R_{D,exa,j}} - \hat{R_{D,red,j}}\right\}^T K \left\{\hat{R_{D,exa,j}} - \hat{R_{D,red,j}}\right\}}{\left\{\hat{R_{D,exa,j}}\right\}^T K \left\{\hat{R_{D,exa,j}}\right\} + \left\{\hat{R_{D,red,j}}\right\}^T K \left\{\hat{R_{D,red,j}}\right\}} \quad (15)$$

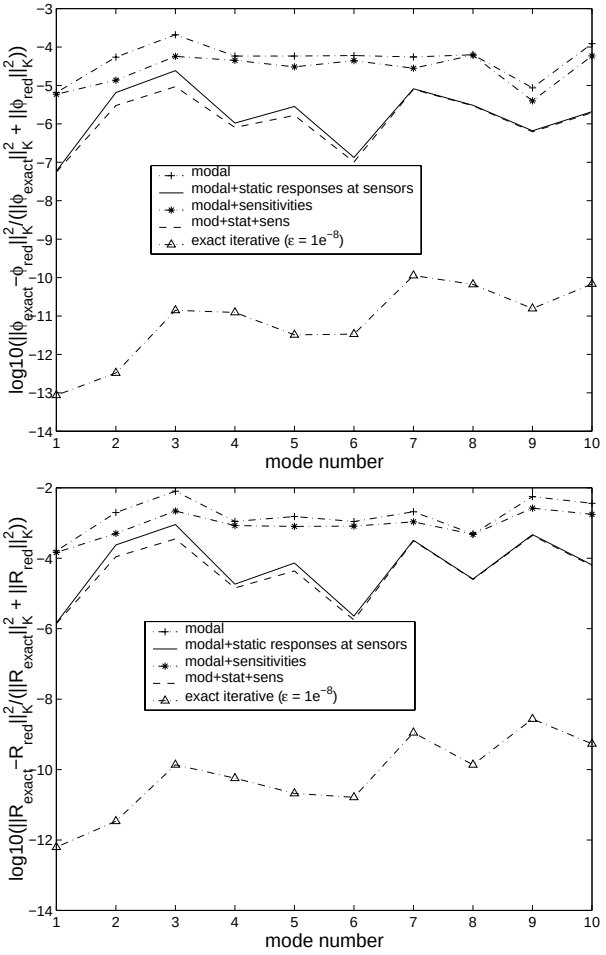

Figure 3: Comparisons of expansion results for the Garteur Model. Top: Shape comparison, see (14), Bottom: Residual comparison, see (15)

A reason to define the relative strain energy of the displacement residuals is that it will be used in the next section of error localization.

Equivalent criterion can be defined with kinetic energy instead of strain energy, but since the results obtained are very similar, they are not presented.

Figures 3 and 4 show the comparisons for the Garteur and engine cover models respectively. With reduced bases, the errors on shape are always lower than those on residues. As expected, adding vectors to the reduced basis improves results. Adding static responses to loads applied at sensors, which leads to an hybrid between modal and static expansion [7], always lead to a significant improvement whereas adding the sensitivities (mod+stat+sens) is only useful for the engine cover case. Finally the comparisons between the iterative and direct methods show that the iterative method has converged indeed.

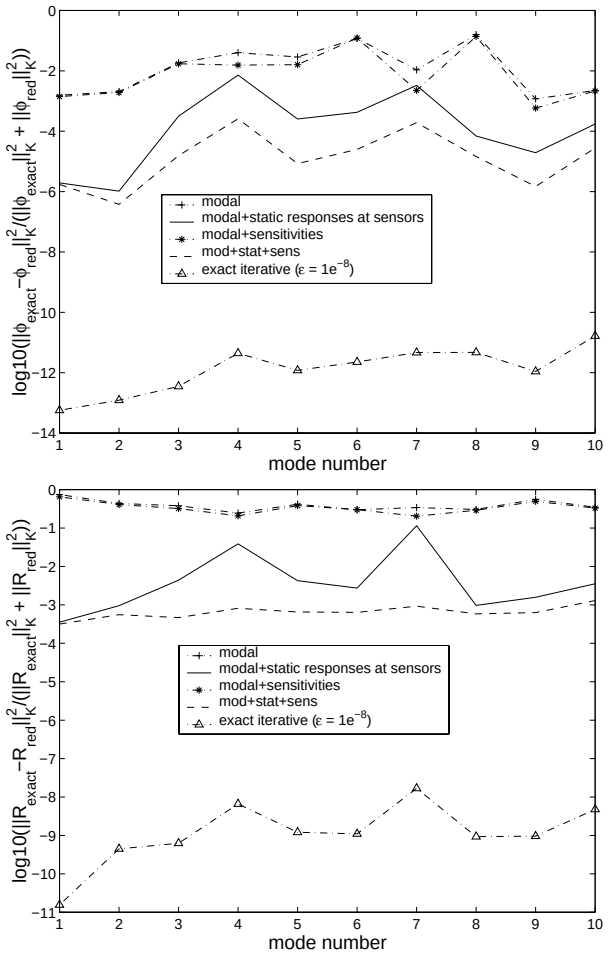

Figure 4: Comparisons of expansion results for the engine cover model. Top: Shape comparison, see (14), Bottom: Residual comparison, see (15)

The next question is to analyze the convergence of the iterative procedure. Figure 5 shows, for the engine cover, the evolution of basis size and relative strain energy error during iterations. A modal basis containing the 20 first modes computed for the

nominal structure (without modification) is used as a starting point even though it was shown earlier than modal+static would have been more appropriate. For the chosen tolerance ϵ of 10^{-6}, convergence is clearly quite rapid. As expected, convergence on the residue is slower.

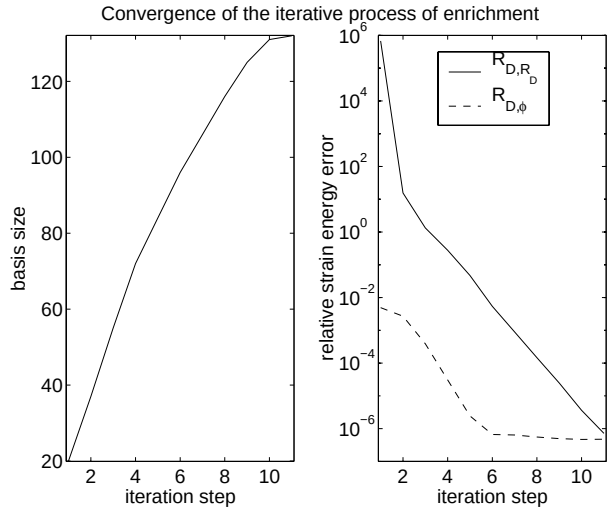

Figure 5: Convergence of the enrichment iterative process, case of the engine cover with the modification of figure 2 ($T_0 = [\phi_{nom,1..20}]$, $tol = 10^{-6}$, γ_j such that $\sigma_j = 10\%$)

Finally, the choice between the various methods will eventually depend on computational times. For the engine cover with $\epsilon = 10^{-8}$ and $\gamma = 10^8$, table 1 shows various computational times.

The main result is that the exact iterative method is tremendously less expensive than the direct method in time (speedup of 72) and required memory (factor 4 with poor code optimization in the case of the iterative method). An additional very interesting fact is that iterating does not significantly add to the required resources when compared to the modal+static solution.

The iterative exact method thus clearly appears as providing the best speed/accuracy compromise.

TABLE 1: summary of computational times (Engine cover, R10000 processor)

Computation of	**iterative exact** $\epsilon = 10^{-8}$	**direct exact**
$\phi_{1:20}$	84 sec	"
$\left(\frac{\partial \phi}{\partial p}_{7:20}\right)$	79 sec	"
$\hat{K}^{-1}b$	25 sec	"
$\left[\phi_{1:20} \ \frac{\partial \phi}{\partial p}_{7:20} \ \hat{K}^{-1}b\right]$	4 sec	"
projection of model	5 sec	"
enrichment	231 sec	"
total	**7.1 min**	**516 min**
Memory	**400 Mo**	**1.6 Go**
Matrix size	**266**	**33680**

4 USING MDRE RESULTS FOR LOCALIZATION

4.1 Localization with the exact residual

One of the main motivations for using MDRE is its theoretical ability to localize defaults. Ideally, MDRE will result in an approximation of the exact residual

$$R_D = \hat{K}^{-1}\big(Z\phi_{mod}\big), \tag{16}$$

where ϕ_{mod} are the modes of the modified structure.

For the case of the engine cover, the mean element strain energy ratio for the exact residual of the first 10 modes

$$e^{el} = \frac{1}{10}\sum_{j=1}^{10} \frac{R_{D,j}^T K^{el} R_{D,j}}{\phi_j^T K \phi_j} \tag{17}$$

is computed and shown in 6 where the localized nature of the exact residual is clearly apparent, showing that localization is feasible using such an indicator (e^{el}). Similar results are obtained for Garteur.

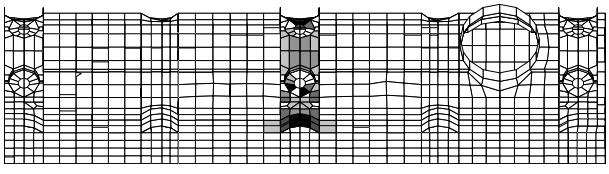

Figure 6: Localization of a modification introduced in the middle, repartition of e^{el} see (17)

4.2 Localization with the MDRE residual

One now considers the displacement residual resulting of the iterative solution of MDRE (with a tolerance of 10^{-8}), and uses it for localization.

The selection of the modeling/measurement error factor γ is a key aspect of using MDRE, since localization will be highly dependent on its value.

Indeed, γ must be high enough in order for the expansion process to take into account the pseudo-measures. Figures 7 and 8 show the effects of γ on localization ability. The following quantities

- $E_{modif} = \frac{1}{10}\sum_{j=1}^{10} \frac{\|R_{D,j}\|^2_{K_{modified\ substructure}}}{\|R_{D,j}\|^2_K}$, which is the ratio between the residual strain energy in the modified substructure and the total residual strain energy,
- $E_{rel,res} = \frac{1}{10}\sum_{j=1}^{10} \frac{\|R_{D,j}\|^2_K}{\|\phi_j\|^2_K}$, which is the relative residual strain energy in the structure,
- $\frac{J_1}{J_2} = \frac{1}{10}\sum_{j=1}^{10} \frac{\|R_{D,j}\|^2_K}{\gamma_j \left\|\{y_{Test,j}\} - [c]\{\phi_{exp,j}\}\right\|^2_{Q_j}}$, which is the ratio between the first and the second term of the cost function (equation (4)),

are plotted versus the relative error on the measured modes σ (γ being computed iteratively such that the desired value of σ is reached, see section 2).

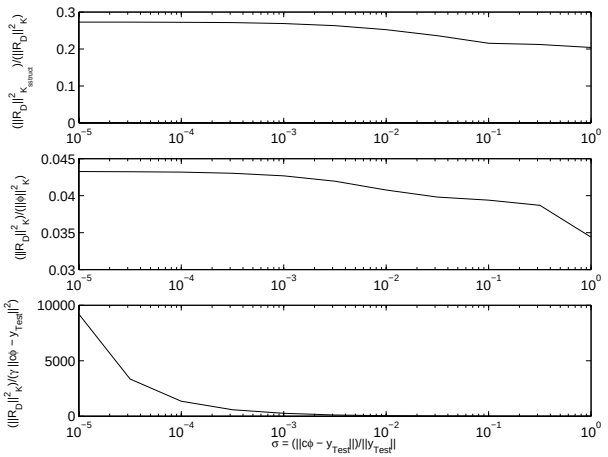

Figure 7: Evolution of different quantities with respect to the relative error on measures (Garteur)

For the Garteur case, figure 7 shows that for a low value of σ, E_{modif} is relatively low (the modified substructure being global and in contact with many other substructures, so that the error spreads to the connected substructures), and decreases slowly when σ increases, indicating a poorer localization for high σ. The relative residual strain energy $E_{rel,res}$ decreases with increasing σ, showing that when one do not take into account measurements information, expansion only searches to minimize the error linked to the model and thus produces a low error with no link to measures. This is confirmed by the study of $\frac{J_1}{J_2}$ which clearly indicates that model-linked error becomes negligible with respect to test-linked error for increasing σ.

For the engine cover (figure 8), the shape of the plots is very similar and brings the same conclusions. The major difference is that E_{modif} is about .5 for low σ, which is higher than for Garteur (the modification is far more local and have less connected substructures, so that the error spreads less).

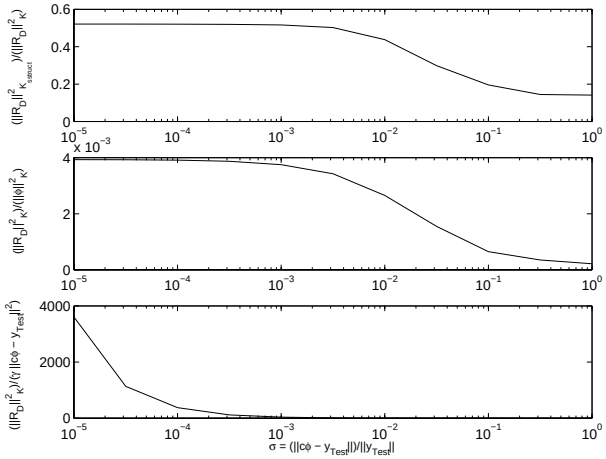

Figure 8: Evolution of different quantities with respect to the relative error on measures (Engine Cover)

Figures 7 and 8 indicate a threshold value for σ, after which localization is no longer possible (because E_{modif} is too low). For the Engine Cover, this value is around 1%, which means that if measurements were performed with more than 1% of error, localization would not be possible. This statement is confirmed by figure 9, which represents the repartition of e^{el} through the Engine Cover model for $\sigma = 10^{-3}$ and $\sigma = 10^{-1}$ respectively. It is clear that allowing 10% error on measures makes localization impossible, whereas a smaller value allows it.

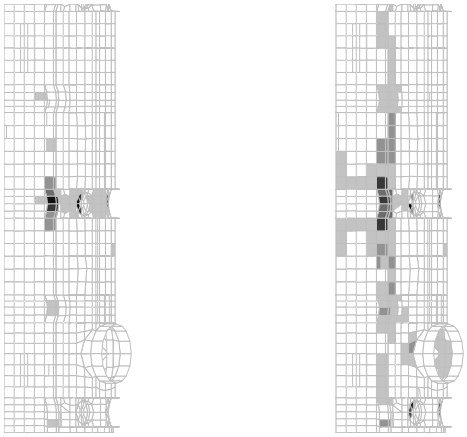

Figure 9: e^{el} **for** $\sigma = 10^{-3}$ **and** $\sigma = 10^{-1}$**, respectively**

Figure 10 represents localization results for Garteur and a low σ (10^{-5}). The quantities plotted are respectively

- e^{el} (see (17)) which is plotted on each element, and
- $e^{node} = \text{diag}([K])^{-1} \frac{1}{10} \sum_{j=1}^{10} \left\{ {R_{L,j}}^2 \right\}$ (term by term square of the dynamic residual) which represents a nodal residual strain energy.

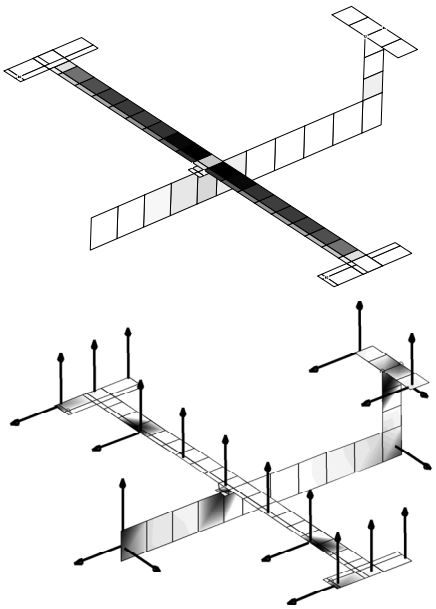

Figure 10: Top: e^{el}**,bottom:** e^{node}

One can see that for a low σ, localization is possible, even if in this case the error spreads to the connected substructures, due to the implicit use of K^{-1} in the two-field formulation (8). It should be noted that for the same value of σ, e^{node} tends to localize error at sensors, which seems to be a constant pattern of MDRE and a drawback for its use in localization.

5 CONCLUSION

The main result of this paper is the introduction of an iterative solver for the full order MDRE problem. The ability to solve the problem exactly on industrial size problems allowed studies on the ability to localize errors using the displacement residual associated with the MDRE solution. The conclusions, drawn from the cases treated, are that the ability to localize is very much dependent on the quality of measurements and that the result has a strong tendency to localize errors on sensors. For uses on real test results, it thus seems essential to run simulations to quantify the ability to localize a given defect before using an MDRE result to draw conclusions on the model.

REFERENCES

[1] **Kammer, D.**, *Test-Analysis Model Development Using an Exact Modal Reduction*, International Journal of Analytical and Experimental Modal Analysis, pp. 174–179, 1987.

[2] **O'Callahan, J., Avitabile, P.** and **Riemer, R.**, *System Equivalent Reduction Expansion Process (SEREP)*, IMAC VII, pp. 29–37, 1989.

[3] **Guyan, R.**, *Reduction of Mass and Stiffness Matrices*, AIAA Journal, Vol. 3, pp. 380, 1965.

[4] **Kidder, R.**, *Reduction of Structural Frequency Equations*, AIAA Journal, Vol. 11, No. 6, 1973.

[5] **Kammer, D.**, *A Hybrid Approach to Test-Analysis Model Development for Large Space Structures*, Journal of Vibration and Acoustics, Vol. 113, No. 3, pp. 325–332, 1991.

[6] **Roy, N., Girard, A.** and **Bugeat, L.-P.**, *Expansion of Experimental Modeshapes - An Improvement of the Projection Technique*, IMAC, pp. 152–158, 1993.

[7] **Balmès, E.**, *Review and Evaluation of Shape Expansion Methods*, IMAC, pp. 555–561, 2000.

[8] **Chouaki, A., Ladevèze, P.** and **Proslier, L.**, *Updating Structural Dynamic Models with Emphasis on the Damping Properties*, AIAA Journal, Vol. 36, No. 6, pp. 1094–1099, June 1998.

[9] **Balmès, E.**, *Optimal Ritz vectors for component mode synthesis using the singular value decomposition*, AIAA Journal, Vol. 34, No. 6, pp. 1256–1260, 1996.

[10] **Chouaki, A.**, Recalage de Modèles Dynamiques de Structures avec Amortissement, Doctoral dissertation LMT/ENS Cachan, 1997.

[11] **Balmès, E.**, Structural Dynamics Toolbox 4.0 (for use with MATLAB), International Technologies, http://www.sdtools.com, 2000.